Int. J. Electrochem. Sci., 11 **(2016)** 10690 – 10705, doi: 10.20964/2016.12.46

International Journal of
ELECTROCHEMICAL
SCIENCE
www.electrochemsci.org

Inhibition Film Formed by 2-mercaptobenzothiazole on Copper Surface and Its Degradation Mechanism in Sodium Chloride Solution

J. Li, C. W. Du[*], *Z. Y. Liu, X. G. Li, M. Liu*

Corrosion and Protection Center, University of Science and Technology Beijing, Beijing 100083, China
[*]E-mail: dcw@ustb.edu.cn

Received: 20 August 2016 / *Accepted:* 28 September 2016 / *Published:* 10 November 2016

Copper surface was modified by 2-mercaptobenzothiazole (MBT) dissolved in isopropanol for the first time. The interaction between MBT and copper, the corrosion inhibition effect of film formed by MBT on copper surface together with its dynamic evolution in 3.5 wt% sodium chloride solution were investigated by Auger electron spectrum (AES), ex-situ Raman spectrum, open circuit potential, potentiodynamic polarization, cyclic voltammograms, electrochemical impedance spectroscopy tests, and scanning electron microscope (SEM). The results of AES and Raman spectrum show that MBT is prone to interact with copper surface to form a complex film consisting of $[Cu(I)MBT]_n$ (having probably polymeric nature) in isopropanol which would oxidize to degrade to form $Cu(II)$ species and $(MBT)_2$ with immersion time extending in the presence of oxygen. The electrochemical tests and SEM indicate the complex film improves corrosion resistance of copper to the media containing chloride by inhibiting both anodic and cathodic reactions with interfering the transport of $CuCl_2^-$ and O_2, and the inhibition effect of $[Cu(I)MBT]_n$ complex film weakens due to its oxidative degradation with immersion time increasing.

Keywords: copper; 2-mercaptobenzothiazole; corrosion inhibition; electrochemical tests; surface characterization

1. INTRODUCTION

With copper being applied in more and more areas, particularly owing to electrical properties, its corrosion in corrosive media becomes a severe problem. One of the effective methods to protect copper against corrosive environments is using inhibitors. The principal inhibitors are 1,2,3-benzotriazole (BTA) and its derivatives [1-4] that are supposed to react with copper cations to form the

coordination compounds. A great number of works have been devoted to investigation of interaction between BTA and its derivatives and copper surface, but that between 2-mercaptobenzothiazole (MBT) and copper is studied to a small extent. MBT has a pK_a of 6.93 at 20 ℃ and hence is present in acid media as the unionized protonated form (HMBT) which could adopt either the thione or the thiol structure [5], as shown in Figure 1. In alkaline media, MBT exists as the thiol ions (MBT^-).

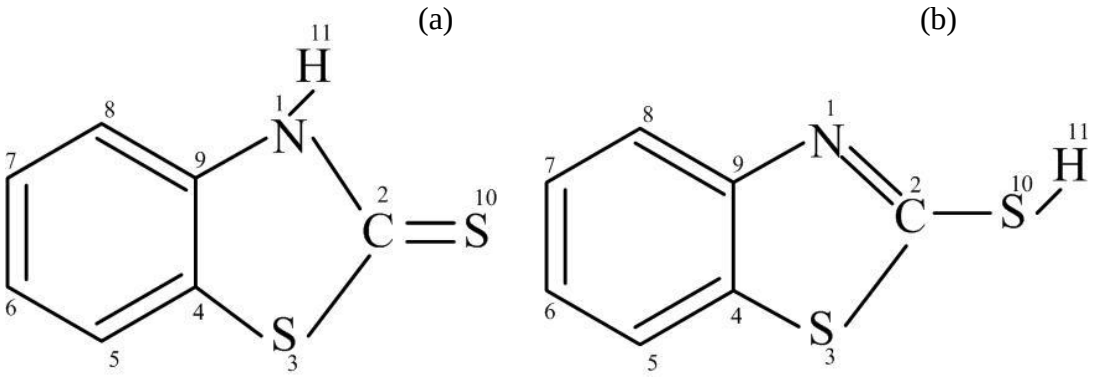

Figure 1. The schematic molecular geometries of thione (a) and thiol (b) forms of MBT.

MBT and its derivatives as corrosion inhibitors of copper and its alloys in various environments were investigated in References [6-17], most of which considered that in all conditions MBT reacts with $Cu(I)$ cations to form a surface film of a complex $Cu(I)$:MBT=1:1. At more positive potentials MBT could be oxidized to 2,2'-dibenzothiazole disulfides. For example, Marciano et al. [18] investigated the effect of MBT on copper corrosion in water-ethanol solution with 0.01 M $HClO_4$ added by means of voltammetry and Raman spectrum. They found that oxidation of MBT would lead to forming a film on the copper surface that inhibits dissolution of copper. Raman spectrum shows the formed film consists of polymeric complex containing copper cations and the ionized form of thiol. However, there exist some contradictory views to the nature of the film formed by MBT on copper surface. Woods et al. [19] observed the surface enhanced Raman scattering (SERS) spectrums for copper electrodes at controlled potentials in a sodium tetraborate solution (pH 9.2), and in the acetate buffer (pH 4.6), both containing MBT. They found that for alkaline media an absorbed layer of MBT occurs in the whole potential range, but for the acidic the initial absorbate is HMBT when potentials ≤ -0.1 V vs. SHE involving π-bonding between the surface and the aromatic ring of the HMBT molecule and as the potential increases, oxidative charge transfer between the electrode and absorbate occurs with the removal of hydrogen atom from the nitrogen to form a hydrogen in solution and with MBT absorbed on copper surface in the form of thiol ion.

Analogously, Huo et al. [20] studied the interaction between MBT and copper surface using electrochemical surface-enhanced infrared reflection absorption spectrum and considered that it is potential dependent as well. Their results indicated that the MBT molecules are absorbed on copper surface vertically as thiolate through exocyclic S atoms at potentials more negative than 0 V vs. SCE, while at more positive potentials electrons transfer between MBT and copper substrate occurs which means that MBT could interact with copper surface to generate a complex film that has polymeric

properties. The formed compact protecting layer could hinder copper dissolution. In conclusion, the interaction between MBT and copper surface and the corrosion inhibition effects of formed surface film are dependent on the solution conditions, such as electrode potential and pH.

Within the frame of present study, it was for the first time that copper surface was modified by MBT dissolved in isopropanol. The characterization of film formed by MBT in on copper surface and its corrosion inhibition effect on corrosion of copper in neutral 3.5 wt% sodium chloride solution were investigated with Auger electron spectrum, ex-situ Raman spectrum, electrochemical tests, and scanning electron microscope. It should be pointed out that the isopropanol is usually used as solvent for modification of copper surface [21]. In addition, the dynamic evolution of the surface film in sodium chloride solution was also researched here which is crucial to its corrosion inhibition effect but has been scarcely conducted in previous investigations.

2. EXPERIMENTAL

2.1 Preparation of solutions and samples

All reagents used in present research were analytical. 2-mercaptobenzothiazole (MBT) was dissolved in isopropanol at a concentration of 0.005 M with a further addition of 40 mL/L of glacial acetic acid which was applied to modification of the copper surface. The acetic acid was included to act as a final etchant to any small quantities of oxide that formed during rinsing and drying. The 3.5 wt% sodium chloride solution prepared with commercial sodium chloride with no further purification and deionized water was employed to observe the corrosion inhibition effect of the surface film formed by MBT on corrosion of copper. Copper samples were embedded in epoxy resin mould leaving a cross-section of 10 mm × 10 mm exposed. Prior to modification or test, the copper surface was ground with silicon carbide abrasive papers of decreasing particle size to #7000, polished with 0.5 μm diamond to mirror surface, rinsed with deionized water, degreased with isopropanol, dried in a stream of compressed air, and then immersed immediately in modification or test solution. Surface modification time set as 2 hr. After modification, the sample was taken out and the copper surface was rinsed and dried as above and then immersed in test solution as soon as possible.

2.2 Characterization of surface

Auger electron spectrum depth profile of the MBT modified copper surface was obtained using PHI-700 nano scanning Auger system (ULVAC-PHI Co.) with sputtering rate being 3 nm/s. Raman spectrums of MBT and the film formed by MBT on copper surface without immersion or immersion for 1, 3, 5 hr were obtained with a Renishaw Raman spectrograph (multichannel compact Raman analyser) that has a rotary encoded grating stage and an internal two stage peltier cooled (−70 ℃) CCD detector. The spectral resolution was 2 cm^{-1} and the wavenumber reproducibility 0.2 cm^{-1}. The incident radiation was conveyed from a He-Ne laser of 632.8 nm excitation through a fibre optic Raman probe. Raman spectrums were recorded at a power of about 5 mW. The morphology of the bare

and surface-modified copper specimens after immersion for 4, 8, and 12 hr in sodium chloride solution were observed via scanning electron microscope (SEM, Quanta 250).

2.3 Electrochemical tests

Electrochemical tests were performed in a conventional three-electrode cell open to air under stagnant conditions at room temperature. The bare or surface-modified copper electrode pretreated as above was used as a working electrode. A saturated calomel electrode (SCE) was used as a reference electrode along with a platinum mesh as a counter electrode. All the following potentials refer to the SCE scale unless marked specially. Tests were carried out with PARSTAT 2273 advanced electrochemical system.

The corrosion potentials of bare and surface-modified copper electrodes in 3.5 wt% sodium chloride solution were measured for immersing to 12 hr. Potentiodynamic polarization tests were performed after immersing the bare and surface-modified samples in sodium chloride solution for different time. Measurements started at −0.25 V vs. the open circuit potential (OCP) and swept to more positive potential with a scan rate of 0.5 mV s^{-1}. The cyclic voltammograms were obtained through linear potential sweep from OCP to the pre-set positive vertex potential, 1 V, and then from the positive vertex potential to the designated negative vertex potential, −1 V, and finally backward to OCP with a scan rate of 20 mV s^{-1} with total 5 cycles after immersing the samples in 3.5 wt% sodium chloride solution for 1 hr. Electrochemical impedance spectroscopy (EIS) measurements were performed at OCP in the frequency range from 100 kHz to 5 mHz with an excitation of a sinusoidal wave of 5 mV amplitude after various immersing times. The impedance data were analyzed with the ZSimpWin impedance software on the basis of equivalent electrical circuits (EEC). All tests were performed for three times in parallel.

3. RESULTS AND DISCUSSION

3.1 Auger electron spectrum (AES)

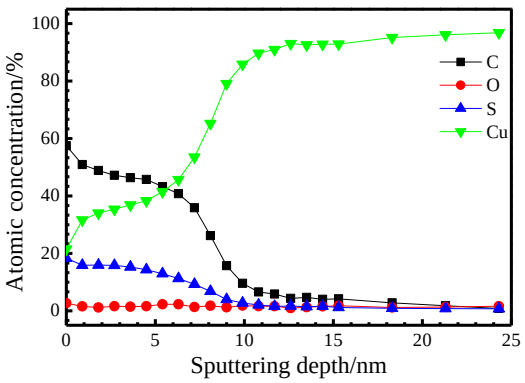

Figure 2. AES depth-profile of copper after surface-modified by MBT dissolved in isopropanol at a concentration of 0.005 M with a further addition of 40 mL/L of glacial acetic acid for 2 hr.

Figure 2 shows AES depth-profile of copper with surface-modified by 2-mercaptobenzothiazole (MBT) dissolved in isopropanol for 2 hr. S and C contents decrease with sputtering depth and the ratio of atomic concentration of S to that of C remains approximately 2:6 which is consistent with molecule components of MBT. The content of Cu is not equal to 0 at the surface and increases with sputtering depth. The above proves that a film consisting of MBT and Cu was formed on copper surface after modification. The content of characteristic element, S, approaches approximately to 0 and the content of Cu to 90% at about 10 nm so that the thickness of surface film could be determined as 10 nm. Besides, the content of O is very low through the whole film even at the interface between film and copper substrate, which confirms that the acetic acid added in isopropanol etched any small quantities of oxide that formed during rinsing and drying indeed as expected.

3.2 Ex-situ Raman spectrum

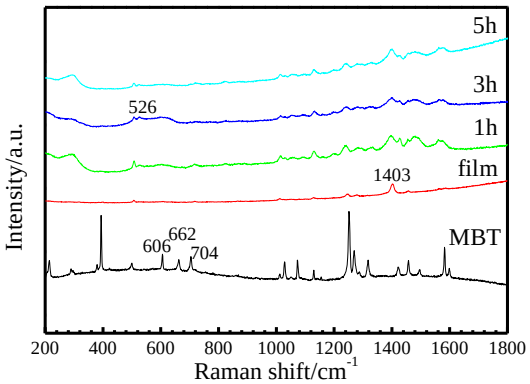

Figure 3. Raman spectrums of MBT in pure powder and the film formed by MBT on copper surface with no immersion and immersing for 1, 3 and 5hr in 3.5 wt% sodium chloride solution.

Ex-situ Raman spectrums were performed to determine the nature of film formed by MBT on copper surface and its evolution in sodium chloride solution. For comparison, the Raman spectrum of MBT in pure powder is shown in Figure 3 as well. MBT could exist in thiol or thione form [22]. In spectrum of MBT, the C-S region shows three bands at 704, 662, and 606 cm^{-1}. According to previous theoretical calculations of the thiol geometry by Sandhyarani et al. [5], three possible C-S vibrations would occur that are ascribed to C_4-S_3, C_2-S_3, and C_2-S_{10} respectively in increasing order of frequency (see Figure 1(b) for the structure). In the thione geometry, the C-S vibrations occur at significantly different positions. The first two bands are due to C_2-S_3 and C_2-S_{10} stretches respectively in decreasing order of frequency, and the third frequency is due to C_4-S_3 vibration. An additional C-S stretch at 486 cm^{-1} is predicted for the thione geometry. This also conforms to the results by Lee and coworkers [23]. It follows that MBT used in present research exists in its thiol form. Compared with the pure MBT, the spectrum of film formed by MBT on copper surface looks largely different and it shows the band characteristics of bulk $Cu(I)MBT$ [19], as shown in Figure 3. The most intense band at 1403 cm^{-1} could be assigned to N_1-C_2-S_3 ring stretch. In Refence [19], Woods et al. thought of that MBT chemisorbs on copper instead of forming $Cu(I)MBT$, though the SERS spectrum of surface film

resembles that of $Cu(I)MBT$. They considered the redshift of some main spectrum bands as a characteristic of chemisorption and due to either dissociative chemisorptions or metal-absorbate charge transfer [23,24]. In present study, it could be concluded that $Cu(I)MBT$ complex film is formed on copper surface in isopropanol instead of MBT chemisorbing on it based on the aforesaid results of AES.

With immersing time extending, Raman spectrum of the surface film varies observable as shown in Figure 3. The characteristic band at 526 cm^{-1} that can be assigned to the disulfide bond [19,25,26], -S-S-, appears apparently, especially after immersing for 3 hr. According to Chadwick et al. [8], $Cu(I)MBT$ could undergo an oxidative dimerization to the form $Cu(II)$ and $(MBT)_2$ which would lead to the degradation of the polymeric complex film formed by MBT on copper surface.

3.3 Electrochemical tests

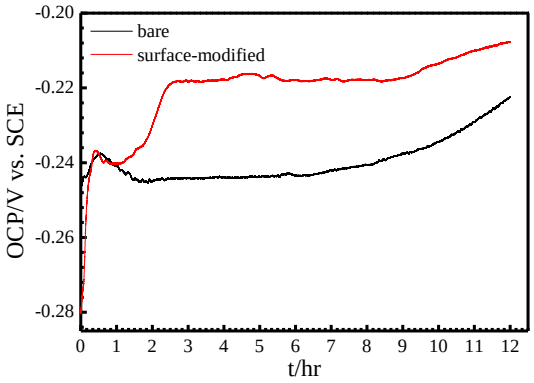

Figure 4. Open circuit potential vs. immersing time plots of the bare and surface-modified copper electrodes in 3.5 wt% sodium chloride solution.

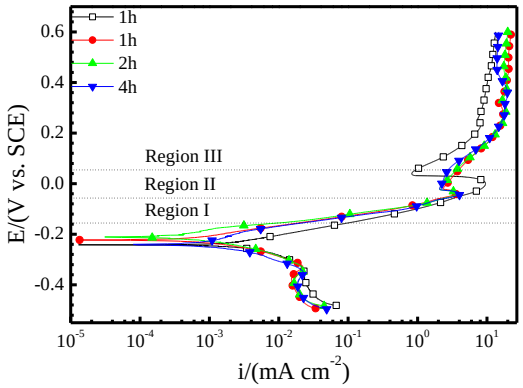

Figure 5. Polarization plots of the bare copper electrode after immersing for 1 hr and the surface-modified after immersing for 1, 2, 4 hr in 3.5 wt% sodium chloride solution with a scan rate of 0.5 mV s^{-1} (hollow icon for the bare and the solid for surface-modified).

The open circuit potentials (OCP) of bare and surface-modified copper electrodes in sodium chloride solution are shown in Figure 4. Compared with that of bare copper electrode, the initial

electrode potential of the modified is more negative which implies the deactivation effects of inhibition film formed by MBT on copper dissolution, and fluctuation is much slighter which reflects that the bare copper electrode surface experiences continuous activation and deactivation processes but the modified is more stable. After about 3 hr, OCP of the surface-modified copper electrode becomes stable and it is more positive than that of the bare. This would be explained below.

Table 1. Corrosion parameters determined by Tafel extrapolation method for the bare and surface-modified copper electrodes in 3.5 wt% sodium chloride solution after immersing for various time.

Immersing time		E_{corr} /(mV)	i_{corr} /($\mu A\ cm^{-2}$)	β_a /(mV $decade^{-1}$)	β_c /(mV $decade^{-1}$)
bare	1h	−242.0	4.9	62.2	126.2
modified	1h	−222.8	2.4	54.2	103.8
	2h	−210.4	2.5	50.0	123.9
	4h	−240.0	2.7	59.3	107.9

A lot of works have been devoted to investigate the mechanism of copper dissolution in chloride-containing media. In near-neutral chloride-containing media with $Cl^- \leq 1$ M, the anodic reaction processes of corroding copper electrode are as follows. First, copper is ionized via an electron transfer under the influence of Cl^- generating CuCl absorbed or deposited on electrode surface:

$$Cu + Cl^- \leftrightarrow CuCl + e^- \quad (1)$$

The CuCl transforms to the soluble cuprous chloride complex, $CuCl_2^-$:

$$CuCl + Cl^- \leftrightarrow CuCl_2^- \quad (2)$$

Then the resultant $CuCl_2^-$, could be oxidized further in accordance with following equations.

$$CuCl_2^- \rightarrow Cu^{2+} + 2Cl^- + e^- \quad (3)$$

$$2CuCl_2^- + 2OH^- \rightarrow Cu_2O + Cl^- + H_2O \quad (4)$$

$$Cu_2O + 1/2\,O_2 + Cl^- + H_2O \rightarrow Cu_2(OH)_3Cl + OH^- \quad (5)$$

Potentiodynamic polarization of the bare and surface-modified copper electrodes in sodium chloride solution results in E vs. i curves shown in Figure 5, and the corresponding corrosion potential (E_{corr}), corrosion currents (i_{corr}), and Tafel slopes determined by the Tafel extrapolation method are listed in Table 1. The cathodic reaction is reduction of oxygen:

$$O_2 + 2H_2O + 4e^- \rightarrow 4OH^- \quad (6)$$

and it could be regarded as being controlled by charge transfer process of the reduction of oxygen close to E_{corr}. Anodic polarization curve could be split into three regions of potential [27], as exhibited by the dotted lines. In region I, an ‘apparent Tafel’ behavior is observed and it is usually assumed the mixed charge transfer and mass transport, predominantly the transport of $CuCl_2^-$ from interface into bulk solution [28], controlling kinetics functions. In region II, CuCl film forms which would result in a maximum peak current density, and subsequent dissolution of the film or metal

would give a limiting current density [29]. With electrode potential more positive, the formation of $Cu(II)$ species and others would give rise to increase in current densities.

As shown in Figure 5, the film formed by MBT on copper electrode surface results in an apparent decrease of the limit diffusion current densities which implies that this film inhibits the transport of oxygen to the interface. However, it has almost no influence on the kinetic process of reduction of oxygen. The anodic current densities of surface-modified copper electrode decrease in aforementioned region I and region II compared with that of the bare, which demonstrates the film hinders dissolution of copper in sodium chloride solution. The combined actions lead to a slightly positive shift of E_{corr}. It's worth noting that in region I, current densities decrease but the apparent Tafel slope remains nearly unchanged which means that this surface film doesn't change the mechanism of charge transfer but inhibits transport of $CuCl_2^-$ merely [27,28]. That's why the potential corresponding to the maximum current density shifts negatively and the maximum current density decreases for the surface-modified copper electrode.

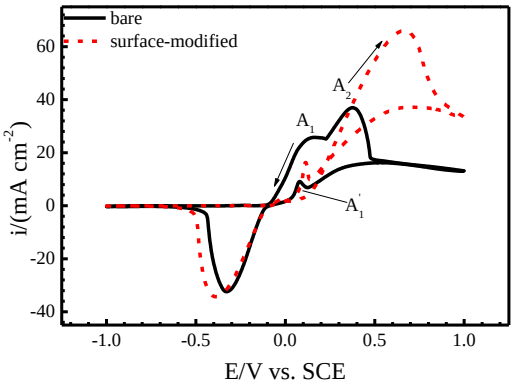

Figure 6. The first cycles of cyclic voltammograms for bare and surface-modified copper electrodes in 3.5 wt% sodium chloride solution after immersing for 1 hr with a linear potential sweep from OCP to the designated positive vertex potential, 1 V, and from the positive vertex potential to the given negative vertex potential, −1 V, and finally backward to OCP at a scan rate of 20 mV s^{-1}.

An interesting phenomenon is current densities increase in region III for surface-modified copper electrode compared with those of the bare and two curves approach each other with electrode potential becoming more positive. Considering that $Cu(I)MBT$ could undergo an oxidative dimerization leading to the formation of $Cu(II)$ and $(MBT)_2$ in the presence of oxygen [8], one reasonable explanation could be proposed as below. With the potential more positive than about 0 V, the next reaction could occur:

$$2Cu(I)MBT \rightarrow 2Cu^{2+} + (MBT)_2 + 4e^- \quad (7)$$

except for

$$CuCl_2^- \rightarrow Cu^{2+} + 2Cl^- + e^- \quad (8)$$

Oxidation of $Cu(I)MBT$ enlarges the current densities observably in region III for the surface-modified copper electrode. This is consistent with conclusion of Woods et al. [19] that MBT^- would be oxidized to $(MBT)_2$ at potentials above about 0.4 V vs. SHE in borate buffer of pH 9.2 according to the following reaction:

$$2MBT^- \rightarrow (MBT)_2 + 2e^- \quad (9)$$

and it could explain why the stable open circuit potential for modified copper electrode is more positive than that of the bare, as shown in Figure 4. With immersing time extending, i_{corr} of the modified copper electrode increases from 2.4 $\mu A\ cm^{-2}$ for 1 hr to 2.7 $\mu A\ cm^{-2}$ for 4 hr which means the protective effect of the complex film formed by MBT on copper surface decreases.

Because from the second cycle on voltammograms are almost invariant and resemble to those of fresh naked copper electrode for both the bare and surface-modified copper electrodes, the first cycle that could reflect the characteristics of surface film (may including corrosion product formed during immersion) is analyzed emphatically. The first cycles of cyclic voltammograms (CVs) of bare and surface-modified copper electrodes after immersing in sodium chloride solution for 1 hr are shown in Figure 6. For the bare case, two oxidation peaks appear at about 0.150 and 0.379 V in the forward scan respectively. The first one, A_1, is ascribed to the formation of CuCl as described by reaction (1,2), and the second one, A_2, is probably due to the oxidation of $Cu(I)$ to soluble $Cu(II)$ species, copper oxide or hydroxychloride according to the aforementioned reactions (3,4,5). In the reverse scan, one small oxidation peak, A_1', occurs at about 0.08 V, which implies that dissolution of copper in sodium chloride solution is reversible, or at least partially reversible [30]. In addition, one large reduction peak appears at −0.32 V corresponding to the reduction of soluble $CuCl_2^-$ in the interface and the CuCl or other $Cu(II)$ species formed during the forward scan and immersion before.

The first cycle of CVs of surface-modified copper electrode in sodium chloride solution exhibits large difference compared with that of the bare. Apparently, the height of A_1 diminishes evidently which implies that the dissolution of copper, i.e., from $Cu(0)$ to $Cu(I)$, is inhibited strongly after surface modification of copper by MBT. Except for that, another phenomenon, the negative shift of the oxidation peak A_1 potential as demonstrated by the arrow, could also be used to confirm the corrosion inhibition effects of the film formed by MBT on copper surface, which has been hardly realized in previous investigations and is interpreted in detail below.

As demonstrated above, the reactions (1,2) are generally considered being reversible and assumed to be under mixed (charge transfer and mass transport controlled) kinetics near to the corrosion potential, i.e., the dissolution of copper in region I is partially reversible. According to the investigations of Nicholson et al. [30,31], for a simplified partially reversible reaction:

$$O + ne^- \leftrightarrow R \quad (10)$$

the difference between oxidation peak and corresponding reduction peak, ΔE_p, is a function of the parameter, φ, and decreases with φ increasing. φ is defined as follow.

$$\varphi = \frac{(D_O/D_R)^{\alpha/2} k^0}{[D_O \pi \upsilon (nF/RT)]^{1/2}} \quad (11)$$

in which D_O, D_R are diffusion coefficients of O and R in the diffusion layer; α is the transfer coefficient; k^0 is the standard rate constant at the standard potential; υ is the sweep rate, dE/dt, and the remaining terms have their usual significance. As mentioned above, the film formed by MBT on cupper surface inhibits the transport of dissolution products, $CuCl_2^-$, probably including the transport of Cl^-. This is equivalent to D_O and D_R decreasing, which would lead to increase of φ. As a result, ΔE_p would decrease. As shown in reaction (1,2), the dissolution of copper in sodium chloride solution is more complex than aforementioned simplified reaction (10). Nevertheless, the fundamental principles are applicative and the final conclusions are analogous. This could be verified by investigation of Benedetti et al [32]. Their results showed that compared with that of stationary electrode the A_1 for rotating disk electrode shifts towards more positive potential except for increase of height in 0.5 M sodium chloride solution because of the accelerating of mass transport by rotating, though they didn't point it out.

It is coincident with the region I and II of potentiodynamic polarization that the height of A_1 diminishes and the corresponding potential shifts negatively, so is A_2 with the region III. As demonstrated by the arrow, the height of A_2 increases and it unlikely results from the oxidation of $Cu(I)$ to $Cu(II)$ species totally, considering that the reaction from $Cu(0)$ to $Cu(I)$ is inhibited strongly as shown by A_1. Hence, the oxidation peak A_2 is ascribed to oxidation of $Cu(I)MBT$ to $Cu(II)$ species and $(MBT)_2$ to a large extent, as shown in reaction (7).

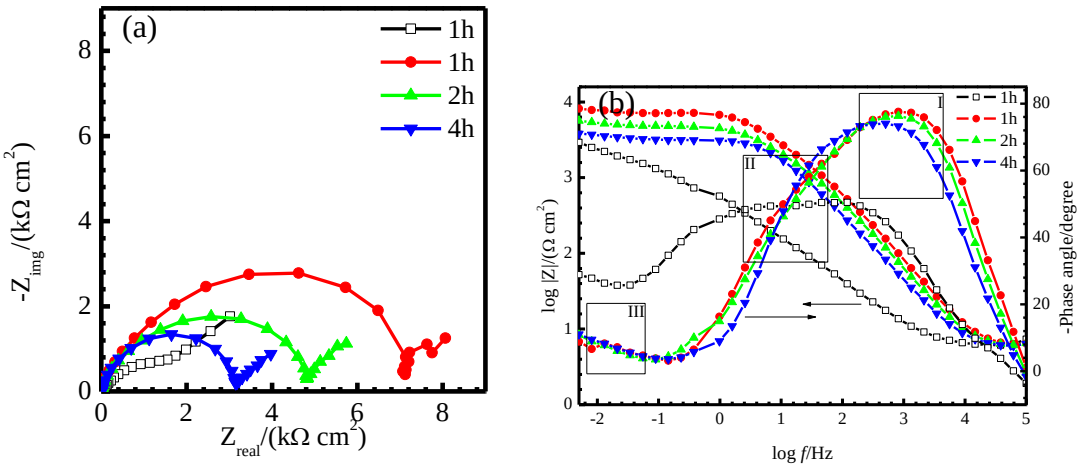

Figure 7. Nyquist (a) and Bode (b) impedance plots for the bare copper electrode after immersing for 1 hr and the surface-modified after immersing for 1, 2, 4 hr in 3.5 wt.% sodium chloride solution with performed at OCP in the frequency range from 100 kHz to 5 mHz under excitation of a sinusoidal wave of 5 mV amplitude (hollow icon for the bare and the solid for surface-modified).

Figure 7 shows the Nyquist (a) and Bode (b) impedance plots for bare copper electrode after immersing for 1 hr and the surface-modified after immersing for 1, 2, 4 hr in sodium chloride solution. Intuitively, the electrochemical impedance for the modified copper electrode is much larger than that

of the bare which means that the film formed by MBT on copper surface indeed inhibits corrosion of copper in sodium chloride solution. This is consistent with aforementioned results of OCP, potentiodynamic polarization, and CVs tests.

In both cases of bare and surface-modified copper electrodes, the Bode plots of EISs show three distinctive segments in Figure 7. The first segment is observed in the high *f* region where log |Z| vs. log *f* reaches a horizontal amplitude and the phase angle approaches 0 with *f* increasing further. This EIS response is typical of a resistor and corresponds to the uncompensated solution resistance, R_{sol}. In the middle *f* region the second segment is observed with a linear relationship between log |Z| vs. log *f* and with the phase angle approaching $-90°$. For that middle *f* region, two relaxation processes could be noted and would be explained below. The third segment is located in low *f* region where |Z| is almost independent of *f* in the log |Z| vs. log *f* spectrum, reaching the so-called dc limit when $|Z| \approx R_p$, the polarization resistance. However, the plateau at low *f* is not completely reached and the phase angle doesn't approach 0 due to the diffusion process.

As mentioned above, three relaxation processes (marked with rectangles in Figure 7(b)) are observed in EISs for both bare and surface-modified copper electrodes, which is also accordant with previous investigations. There exist contradictions to identify the corresponding physicochemical process occurring on the surface for every time constant. A reasonable identification is made by Ingelgem et al [33]. They used broadband impedance spectroscopy of copper electrode in sodium chloride solution and demonstrated that the relaxation I is related to the double layer on the surface containing also information about charge transfer processes, relaxation II represents a parallel combination of two corrosion product layers coexisting on the surface, and relaxation III is associated with mass transport in the solution. This is also consistent with the conclusions derived from Faradaic impedance theory and experimental results obtained by Deslouis et al. [34] that ascribed the capacitive loop at high frequency region to double layer capacitance, C_{dl}, and charge transfer resistance, R_{ct}, that at low frequency region to mass transport, and that at intermediate frequency region to the modulation of CuCl on the surface.

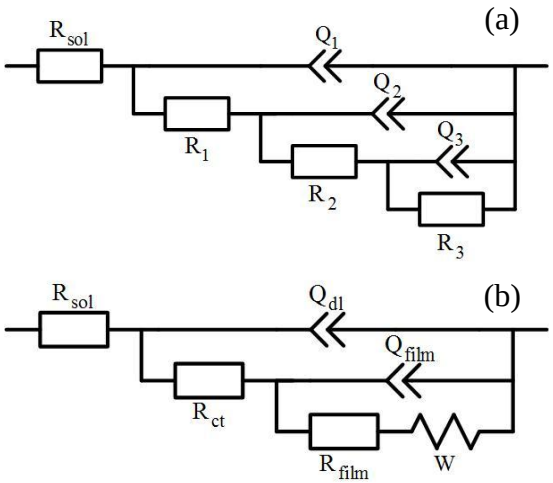

Figure 8. Equivalent electrical circuit models for rotating (a) and stationary (b) copper electrodes in sodium chloride solution.

$R_{sol}(Q_1(R_1(Q_2(R_2(Q_3R_3)))))$ nested equivalent electrical circuit (EEC) which is shown in Figure 8(a) is usually used to fit the EIS response for rotating copper electrode in sodium chloride solution. Based on the discussion above, the $R_{sol}(Q_{dl}(R_{ct}(Q_{film}(R_{film}W))))$ EEC is adopted to fit the experimental EISs in present study, as shown in Figure 8(b). R is the resistance and W represents the Warburg element for the diffusion process. Replacing (Q_3R_3) with W is because when rotation is not present the classical Warburg impedance is applicable to diffusion process instead of the convective Warburg impedance. The symbol Q represents constant phase element (CPE) modeling a non-ideal capacitance whose impedance is defined as:

$$Z_{CPE} = [Q(j\omega)^n]^{-1} \quad (12)$$

The parameter Q and n are independent of the frequency. The value of n could be $0 \leq n \leq 1$ or -1. A value of 1 describes an ideal capacitor, 0 an ideal resistance, and -1 an inductor. Values of n differing from 1 or 0 could be attributed to in-depth, lateral, or time distributions of the observed phenomenon, i.e., the dispersion effect, and when n=0.5 the CPE represents a Warburg impedance.

Table 2. Results obtained by fitting experimental EISs using EEC model in Figure 5(b) for the bare and surface-modified copper electrodes in 3.5 wt% sodium chloride solution after immersing for various time.

Immersing time		R_{sol} /(Ω cm^2)	Q_{dl} /(Ω^{-1} cm^{-2} s^n)	n_{dl}	R_{ct} /(Ω cm^2)	Q_{film} /(Ω^{-1} cm^{-2} s^n)	n_{film}	R_{film} /(Ω cm^2)	W / (Ω^{-1} cm^{-2} s$^{0.5}$)
bare	1h	5.7	2.1×10^{-4}	0.72	227.2	2.3×10^{-4}	0.71	1478	2.4×10^{-3}
modified	1h	5.9	3.0×10^{-6}	0.95	1374	1.3×10^{-5}	0.72	6612	2.6×10^{-3}
	2h	5.8	4.7×10^{-6}	0.93	1599	1.4×10^{-5}	0.82	3109	3.6×10^{-3}
	4h	5.7	7.7×10^{-6}	0.91	1166	5.0×10^{-6}	0.90	1925	4.5×10^{-3}

Table 2 show the fitted parameters when $R_{sol}(Q_{dl}(R_{ct}(Q_{film}(R_{film}W))))$ EEC was employed to simulate the electrochemical response of bare and surface-modified copper electrodes immersing for various time in sodium chloride solution. All of the errors of the fitting parameters are less than 15% which confirms the suitability of the EEC used. The quality of inhibition film could be evaluated by R_{film} and Q_{dl}. R_{film} represents the transfer resistance of charge through the film and Q_{dl} describes the electric double-layer capacitance. Strictly speaking, when there exists a film on copper surface, especially as solid phase, it is more exact that Q_{dl} represents the non-Faradaic charge and discharge capacitance that is related to the interfacial properties. The more densely and thicker the inhibition film, the lager the R_{film} and the lower the Q_{dl}. After modification R_{film} increases from 1478 to 6612 Ω cm^2, which indicates the surface-modified copper is much more corrosion-resistant in media

containing chloride. Besides, Q_{dl} of the surface-modified electrode decreases by about two orders of magnitude from 2.1×10^{-4} to $3.0\times10^{-6}\ \Omega^{-1}\ cm^{-2}\ s^{n}$ compared with those of bare copper electrode. The decrease in Q_{dl} may be attributed to the film formed by MBT on copper surface resulting in an increase in the thickness of the double electrical layer and a decrease in dielectric constant [35]. According to Brug et al. the hypothetical interfacial capacitance, C_{dl}, is related to Q_{dl} as following formula for a faradaic system:

$$C_{dl} = \left[Q_{dl}(1/R_{sol}+1/R_{ct})^{n-1}\right]^{n} \quad (13)$$

The calculated C_{dl} is 2.5 $\mu F\ cm^{-2}$ in the case of immersing for 1 hr. In view of the fact that n_{dl} increases from 0.72 for bare copper electrode to 0.95 for the surface-modified which implies a certain increase of the surface homogeneity due to the modification by MBT [35], C_{dl} could be calculated approximately by the Helmholtz model although the model is rather simplified. The capacitance per unit area is

$$C_{dl}=\frac{\varepsilon_0\varepsilon_{film}}{d_{film}} \quad (14)$$

where d_{film} is the thickness of inhibition film, ε_0 the permittivity of vacuum with the value $8.854187817\times10^{-12}$ F/m, and ε_{film} the relative permittivity of $Cu(I)MBT$ (about 6.29 [37]). The calculated thickness of inhibition film is 2.2 nm with the same order of magnitudes and a little less than the value measured by AES, about 10 nm. The error comes from the inevitable permeation of H_2O into inhibition film in solution that would increase the relative permittivity consequently.

With immersing time extending, R_{film} that could represent the protective effect of the complex film formed by MBT on copper surface decreases. Based on the results of CVs obtained before and that of Chadwick et al. [8] one could conclude the reason why R_{film} decreases is that in the presence of oxygen the $Cu(I)MBT$ complexes undergo an oxidative dimerization resulting in the formation of $Cu(II)$ species and $(MBT)_2$ containing -S-S-, as reaction (7) describes, which would result in the degradation of the polymerization film. This assumption has been evidenced by Raman spectroscopy of the surface film after various immersing times as above. Besides, the corresponding n_{dl} decreases with immersing time extending which results from the increase of surface inhomogeneity due to the degradation of polymerization film.

3.4 Scanning electron microscope (SEM)

Figure 9 shows the SEM images of bare and surface-modified copper surfaces after immersing for various time in sodium chloride solution. After immersing for 4 hr, the bare copper surface has suffered rather severe local corrosion and shallow pits are visible. The granular corrosion products spread over copper surface uniformly and Energy Dispersive Spectrometer (EDS) shows that they contain considerable O and Cl except for abundant Cu. The corrosion products may be Cu_2O and $Cu_2(OH)_3Cl$, and the form of uniformly spreading granules in which they exist could verify the

conclusion by Bengough et al. [22]. They assumed the main initial corrosion product of copper in neutral media containing abundant Cl^- is CuCl formed via reaction (1,2), and CuCl that is slightly soluble in dilute sodium chloride and deposits to form film on surface reacts to produce Cu_2O. The method of producing Cu_2O in the presence of Cl^- is usually taken as not a direct electrochemical or chemical formation from the base metal or CuCl but a precipitation reaction via reaction (4,5).

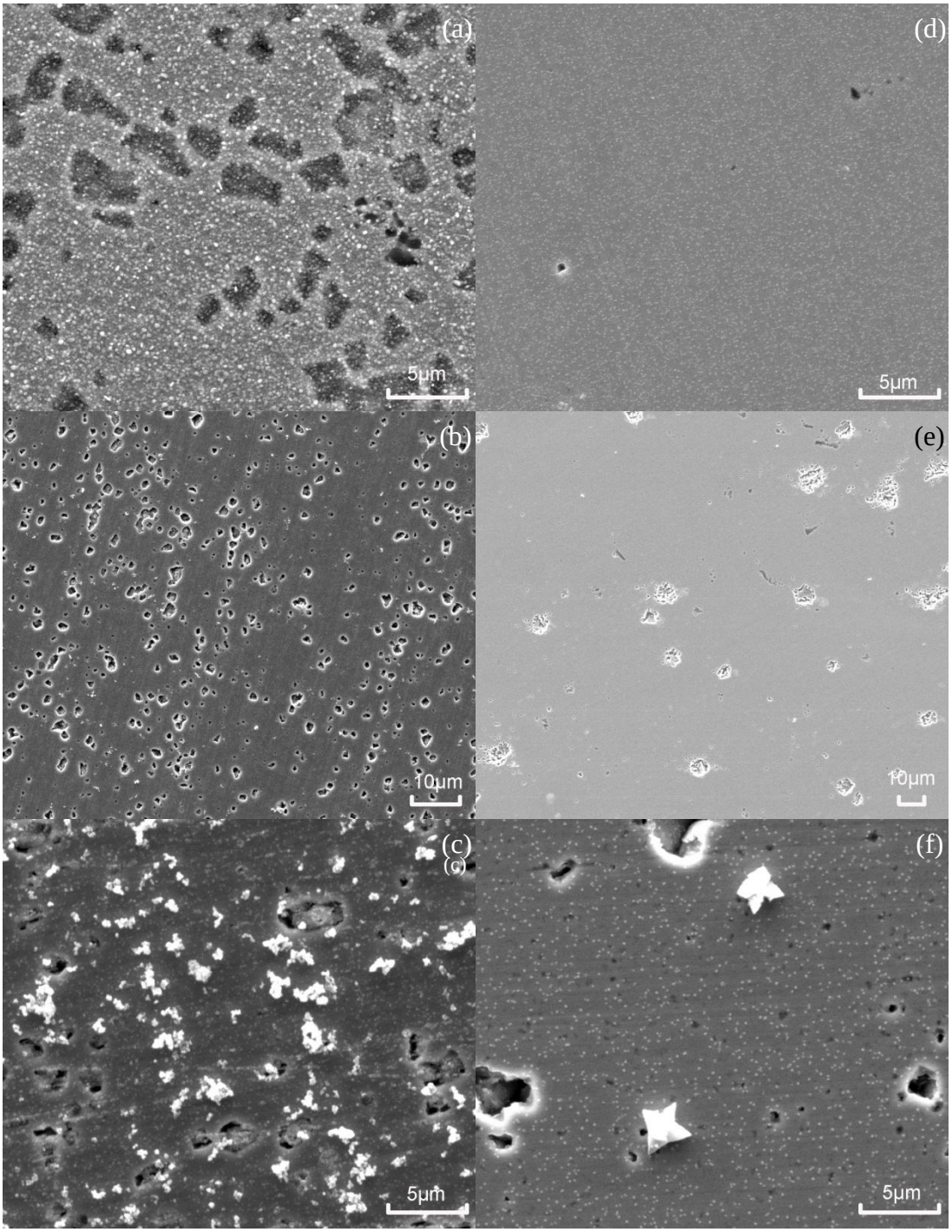

Figure 9. SEM images of the bare (a, b, c) and surface-modified (d, e, f) copper surfaces after immersing for 4 (a, d), 8 (b, e) and 12 hr (c, f) in 3.5 wt.% sodium chloride solution.

The equilibrium in reaction (4) is shifted to the right as the local concentration of the $CuCl_2^-$ complex increases and Cu_2O is deposited in response. Compared with that of bare copper surface, corrosion of the modified copper surface is slighter and the granules of corrosion product are smaller except for some relatively severe local attacks. After immersing for 8 hr, the shallow pits for bare copper surface developed to deep holes and spread densely over the surface. On the contrary, the local attacks for modified copper surface are shallow and spares. When immersing time increased to 12 hr, the local corrosion of bare copper surface is more severe and flocculent products are formed. For the modified copper surface, those mature local pits developed more thoroughly which manifests as vacuum up in the holes, and abundant of unstable local attacks were generated.

The above proves that the modified copper surface is more resistive to corrosion in media containing chlorides, i.e., a corrosion inhibition film was formed on copper surface by MBT dissolved in isopropanol which is consistent with the results of AES, Raman spectrum, and electrochemical tests. With immersing time extending, the inhibition film was degraded by oxygen as shown by Raman spectrum and some local attacks occurred on copper surface.

4. CONCLUSIONS

Assessing the results of electrochemical tests and characterization of surface leads to the following conclusions:

1. MBT is prone to interact with copper surface to form a complex film consisting of $[Cu(I)MBT]_n$ (having probably polymeric nature) in isopropanol.
2. $[Cu(I)MBT]_n$ complex film on copper surface shows inhibition effect on the corrosion of copper in 3.5 wt% sodium chloride solution, and potentiodynamic polarization demonstrated that $[Cu(I)MBT]_n$ complex film inhibits both anodic and cathodic reactions with interfering the transport of $CuCl_2^-$ and O_2.
3. $R_{sol}(Q_{dl}(R_{ct}(Q_{film}(R_{film}W))))$ EES is applicable to corrosion of the bare and surface-modified copper electrodes and R_{film}, the resistance of surface film to charge transport, could represent its corrosion inhibition effects on copper.
4. The inhibition effect of $[Cu(I)MBT]_n$ complex film on copper surface weakens with immersing time increasing due to its oxidation degradation by presence of O_2, which would lead to formation of $Cu(II)$ species and $(MBT)_2$.

ACKNOWLEDGEMENTS
This work was supported by the National Basic Research Program of China (973 Program project, No. 2014CB643300) and the National Science and Technology Infrastructure Platforms Construction Project.

References

1. M. Finšgar and I. Milošev, *Corros. Sci.*, 52 (2010) 2737.
2. M. Mihajlović and M. Antonijević, *Int. J. Electrochem. Sci.*, 10 (2015) 1027.

3. M. Antonijević, M. Snežana and B. Marija, *Corros. Sci.*, 51 (2009) 1228.
4. E. Abdullayev, V. Abbasov, A. Tursunbayeva, V. Portnov, H. Ibrahimov, G. Mukhtarova and Y. Lvov, *ACS Appl. Mat. interfaces*, 5 (2013) 4464.
5. N. Sandhyarani, G. Skanth, S. Berchmans, V. Yegnaraman and T. Pradeep, *J. Colloid Interface Sci.*, 209 (1999) 154.
6. G. Contini, S. Turchini, V. D. Castro, G. Polzonetti and A. M. Marabini, *Appl. Surf. Sci.*, 59 (1992) 1.
7. M. Ohsawa and W. Suetaka, *Corros. Sci.*, 19 (1979) 709.
8. D. Chadwick and T. Hashemi, *Surf. Sci.*, 89 (1979) 649.
9. M. Finšgar and D. K. Merl, *Corros. Sci.*, 83 (2014) 164.
10. Q. Bao, D. Zhang and Y. Wan, *Appl. Surf. Sci.*, 257 (2011) 10529.
11. E. Abdullayev, V. Abbasov, A. Tursunbayeva, V. Portnov, H. Ibrahimov, G. Mukhtarova and Y. Lvov, *ACS Appl. Mat. interfaces*, 5 (2013) 4464.
12. M. Finšgar, *Corros. Sci.*, 77 (2013) 350.
13. M. Musiani, M.G. Mengoli, M. Fleischmann and R.B. Lowry, *J. Electroanal. Chem.*, 217 (1987) 187.
14. L. P. Kazansky, I. A. Selyaninov and Y. I. Kuznetsov, *Appl. Surf. Sci.*, 258 (2012) 6807.
15. G. Brunoro, F. Parmigiani, G. Perboni, G. Rocchini and G. Trabanelli, *Br. Corros. J.*, 27 (1992) 75.
16. J. Izquierdo, J. J. Santana, S. González and R. M. Souto, *Prog. Org. Coat.*, 74 (2012) 526.
17. ESM Sherif, Int. *J. Electrochem. Sci.*, 7 (2012) 1482.
18. J. C. Marconato, L. O. Bulhes and M. L. Temperini, *Electrochim. Acta*, 43 (1998) 771.
19. R. Woods, G. A. Hope and K. Watling, *J. Appl. Electrochem.*, 30 (2000) 1209.
20. S. J. Huo, L. H. CHEN, Q. ZHU Q and J. H. Fang, *Acta Phys. Chim. Sin.*, 29 (2013) 2565.
21. D. A. Hutt and C. Liu, Appl. *Surf. Sci.*, 252 (2005) 400.
22. A. K. Rai, R. Singh, K. N. Singh and V. B. Singh, *Spectrochim. Acta, Part A*, 63 (2006) 483.
23. C. J. Lee, S. Y. Lee, M. R. Karim and M. S. Lee, *Spectrochim. Acta, Part A*, 68 (2007) 1313.
24. A. Otto, I. Mrozek, H. Grabhorn and W. Akemann, *J. Phys.: Condens. Matter*, 4 (1992) 1143.
25. H. E. Van Wart and H. A. Scheraga, *J. Phys. Chem.*, 80 (1976) 1823.
26. M. C. Chen, R. C. Lord and R. Mendelsohn, *J. Am.Chem. Soc.*, 96 (1974) 3038.
27. G. Kear, B. D. Barker and F. C. Walsh, *Corros. Sci.*,46 (2004) 109.
28. W. H. Smyrl, *J. Electrochem. Soc.*, 132 (1985) 1555.
29. O. E. Barcia, O. R. Mattos, N. Pebere and B. Tribollet, *J. Electrochem. Soc.*, 140 (1993) 2825.
30. R. S. Nicholson and I. Shain, *Anal. Chem.*, 36 (1964) 706.
31. R. S. Nicholson, *Anal. Chem.*, 37 (1965) 1351.
32. A. V. Benedeti, P. T. A. Sumodjo, K. Nobe, P. L. Cabot and W. G. Proud, *Electrochim. Acta*, 40 (1995) 2657.
33. Y. V. Ingelgem, E. Tourwé, J. Vereecken and A. Hubin, *Electrochim. Acta*, 53 (2008) 7523.
34. C. Deslouis, B. Tribollet, G. Mengoli and M. M. Musiani, *J. Appl. Electrochem.*, 18 (1988) 384.
35. W. Chen, S. Hong, H. B. Li, H. Q. Luo, M. Li and N. B. Li, *Corros. Sci.*, 61 (2012) 53.
36. J. Wang, B. Z. Zeng, C. Fang and X. Y. Zhou, *Anal. Sci.*, 16 (2000) 457.